

Near-Capacity Detection and Decoding: Code Design for Dynamic User Loads in Gaussian Multiple Access Channels

Xiaojie Wang, *Student Member, IEEE*, Sebastian Cammerer, *Student Member, IEEE*,
and Stephan ten Brink, *Senior Member, IEEE*

Abstract—This paper considers the forward error correction (FEC) code design for approaching the capacity of a *dynamic* multiple access channel (MAC) where both the number of users and their respective signal powers keep constantly changing, resembling the scenario of an actual wireless cellular system. To obtain a low-complexity non-orthogonal multiple access (NOMA) scheme, we propose a serial concatenation of a low-density parity-check (LDPC) code and a repetition code (REP), this way achieving near Gaussian MAC (GMAC) capacity performance while coping with the dynamics of the MAC system. The joint optimization of the LDPC and REP codes is addressed by matching the analytical extrinsic information transfer (EXIT) functions of the sub-optimal multi-user detector (MUD) and the channel code for a specific and static MAC system, achieving near-GMAC capacity. We show that the near-capacity performance can be flexibly maintained with the same LDPC code regardless of the variations in the number of users and power levels. This flexibility (or elasticity) is provided by the REP code, acting as “user-load and power equalizer”, dramatically simplifying the practical implementation of NOMA schemes, as only a single LDPC code is needed to cope with the dynamics of the MAC system.

Index Terms—Interleave division multiple access, EXIT chart, non-orthogonal multiple access, LDPC code, multi-user detection.

I. INTRODUCTION

The fundamental capacity limit of information transmission between one transmitter and one receiver over an additive white Gaussian noise (AWGN) channel, laid down by Shannon, has virtually been achieved. In fact, there exist several powerful and practical codes, e.g., Turbo [1], LDPC [2] and Polar codes [3], that can operate close to capacity with both moderate codeword length as well as feasible decoding complexity. However, the situation changes when considering multi-user setups, such as the multiple access channel (MAC), i.e., multiple transmitters (or users) and one single receiver.

Parts of the results were presented at the International Symposium on Turbo Codes and Iterative Information Processing (ISTC), Hong Kong, December 2018.

The authors are with Institute of Telecommunications, Pfaffenwaldring 47, University of Stuttgart, 70569 Stuttgart, Germany (e-mail: {wang, cammerer, tenbrink}@inue.uni-stuttgart.de).

The MAC capacity (region) has been known since the 1970s [4] and can be determined by a tuple of rates R_k , $1 \leq k \leq N$ of the N individual users. In this paper, we assume that no cooperation is allowed among users, e.g., no power control and/or cooperative encoding at the transmitters. We refer interested readers to [5], [6], [7] for a detailed discussion of capacity regions and different cooperative schemes in multi-user settings. Often, the capacity region is *dominantly* bounded by the sum capacity constraint of all users. These rate tuples, resulting in maximum sum-rate, constitute an *edge* or *facet* in vector space with dimension of two or higher, respectively. It is referred to as *dominant face* of the MAC capacity region, which is of particular practical interest.

To achieve arbitrary points of the *dominant face* (illustrated for the two-user case in Fig. 1), existing approaches rely on joint multi-user decoding or successive interference cancellation (SIC) with time sharing/rate-splitting [8], [9], [10]. Joint decoding is not feasible in terms of complexity even for a small number of users. While SIC can achieve certain corner points of the capacity region, it suffers from high latency and potential error propagation. Moreover if finite block length codes are used, the gap to capacity increases as the number of users grows [11, Fig. 5]. However, due to its theoretically capacity-achieving capability with codeword length approaching infinity, various non-orthogonal multiple access (NOMA) schemes in the literature still apply SIC to delay-insensitive applications [12], [13], [14], [15].

Other orthogonal methods such as time division multiple access (TDMA), frequency division multiple access (FDMA) and code division multiple access (CDMA) avoid interference by providing orthogonal channels so that each user can detect and decode its signal independently. However, these schemes may require, on the one hand, complex synchronization and tracking algorithms to maintain orthogonality in time/frequency/code domain, while, on the other hand, achieve solely one point of the capacity region where optimum resource allocation in terms of bandwidth, power and time is

[33] consider the coding-spreading trade-off and a hybrid MUD to improve convergence, yet only based on a few selected codes and a few number of users. However, the systematic design and optimization of the joint detection and decoding schemes over the multiple-access channel still remains an open problem.

Recent works in [34], [35], [36] address LDPC code design with two users applying optimal joint detection and a Gaussian-mixture model to approximate the message probability density function (PDF) at the CNs. In [37], the LDPC codes are optimized for IDMA systems with a relatively large number of users (6 to 10), again with an optimum joint MUD. In [38], the 5G LDPC code is studied for multi-user communications assuming optimal MUD. This joint MUD eliminates one of the most attractive features of IDMA, namely, its low complexity. Furthermore, for a moderate to large number of users, an optimum joint MUD is computationally prohibitive and, therefore, the code design for such large systems has not yet been adequately addressed, although the design of binary LDPC codes for iterative detection and decoding is well-understood in the EXIT-chart framework [24], [39], [40].

In [41], [42], the authors study the code properties in the MAC setting and optimize irregular repeat and accumulate (IRA) code design for the sub-optimal MUD of IDMA with a fixed number of users and an equal power setting. In [43], [44], low-cost implementations of IDMA are considered and compared to other NOMA schemes, showing the superior performance of IDMA.

C. Contributions

This paper considers a dynamic (uplink) IDMA system with both varying number of users and varying received signal power strength. We seek to find a *simple* and *flexible* coding scheme for coping with the dynamics of the system parameters. The contributions of this paper are summarized in the following.

- We propose to use serially concatenated LDPC and repetition (REP) codes for a dynamic MAC system. We refer to a dynamic MAC system as a model for a real cellular network with constantly changing number of users and varying signal power levels.
- An analytical expression of the EXIT function capturing the LDPC, REP and the sub-optimal MUD is derived.
- A joint optimization of LDPC and REP code is carried out to match the low-complexity MUD in a given (static) MAC system.
- We show that the REP code can be used as “user-load equalizer” to compensate the influence of a varying number of users, i.e., the *same* LDPC code fits different number of active users with hardly any performance loss.

- We show that the REP code can also be used as “power equalizer” to compensate the influence of varying power levels, i.e., the *same* LDPC code fits different power levels with hardly any performance loss.

Simulation results show that we can achieve close to GMAC capacity with 1.28 dB $\frac{E_b}{N_0}$ loss at a sum-rate of 0.9375 bpcu supporting 30 users each with BPSK modulation¹; this performance can be achieved over a wide range of number of users and in equal or non equal-power scenarios by simply varying the repetition code-rate while fixing the LDPC code.

The paper is structured as follows. The IDMA system model and the multi-stage low-complexity iterative receiver is explained in Sec. II. The EXIT functions are subsequently reviewed and elaborated on in the IDMA framework in Sec. III. Then, the joint optimization of the serially concatenated LDPC and REP code is presented in Sec. IV. Sec. V discusses the performance in unequal power scenarios by exploiting the “power equalizer” functionality of the REP code. Finally, Sec. VI concludes this paper.

II. IDMA SYSTEM MODEL

Fig. 2 shows the IDMA system model with N non-cooperative users. Each user encodes and decodes its data separately using an LDPC encoder of code rate of R_c and a serially concatenated repetition code of rate of $R_r = \frac{1}{d_r}$. Note that the code parameters, e.g., degree profile and parity check matrix \mathbf{H} are the same among all the users. The total code rate is $R_{\text{tot}} = R_c R_r$. The interleaver is, on the contrary, user-specific to allow efficient user separation at the receiver. After interleaving, the coded bits are mapped to symbols, e.g., BPSK, and transmitted over a channel.

Consider uncorrelated ergodic Rayleigh fading channels, the m th received signal (i.e., the m th element of \mathbf{y} in Fig. 2) of all users can be written as

$$y_m = \sum_{i=1}^N \sqrt{P_i} h_{i,m} \underbrace{x_{i,m}}_{:=\tilde{x}_{i,m}} \cdot e^{j\varphi_{i,m}} + n_m \quad (1)$$

where m is the discrete-time index, n_m is circularly symmetric (complex-valued) AWGN with zero mean and variance σ_n^2 , $h_{i,m}$ is the uncorrelated (both over time and among different users) small-scale Rayleigh fading channel coefficient, P_i is the received signal power strength of the i th user and $\varphi_{i,m}$ is a pseudo random phase scrambling to avoid ambiguity of the super-constellation (Cartesian product of all users’ constellations). This

¹The target sum-rate is chosen such that the interference and noise have roughly the same impact on the performance. For low SNRs, the performance is mainly noise-limited and single-user coding suffices. For high SNRs, the performance is mainly interference-limited and orthogonal schemes or repetition coding suffice(s); Detailed discussions in Sec. IV-A.

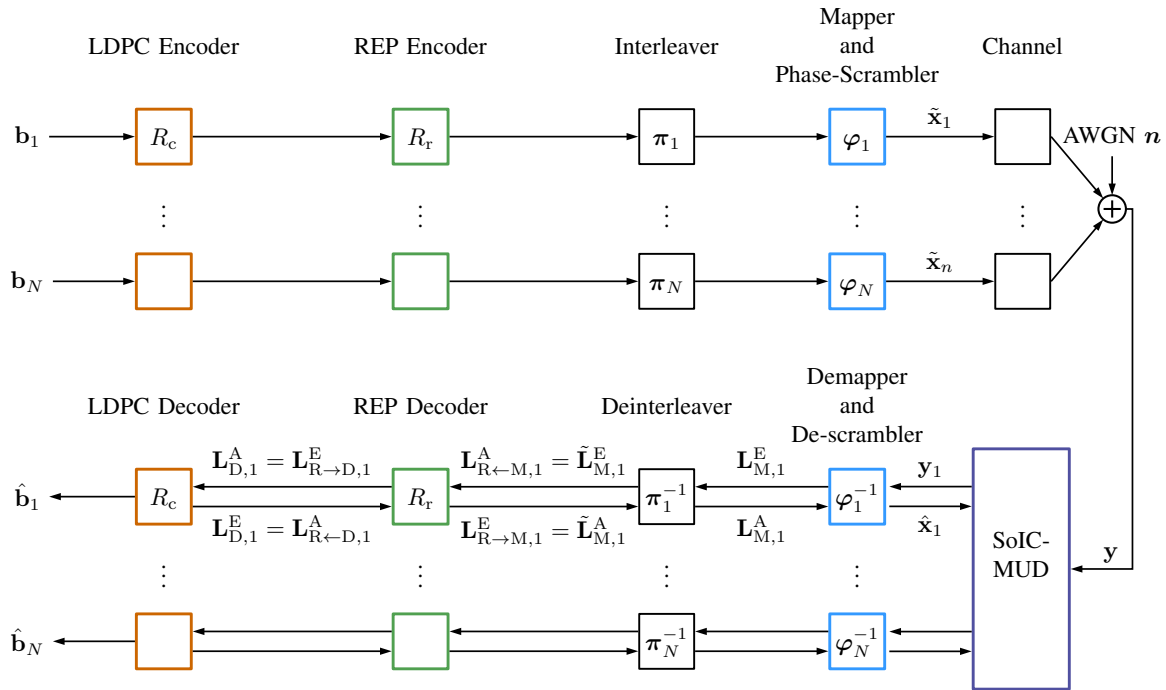


Fig. 2. IDMA system model; all users have the same power/code/modulation; note that boldface letters are used to denote vectors.

random phase shift could also be the consequence of, e.g., the channel and/or explicit “scrambling” and we include this into each user’s mapper (only for AWGN channels; for Rayleigh fading channels, this step can be omitted). Throughout this paper, the phases $\varphi_{i,m}$ are independently and uniformly distributed in $[0, \pi)$. Alternatively, a phase “scrambling”, which is a constant for all symbols but distinct per user, can also be applied (but subject to optimization). The output of the mapper of the i th user with BPSK modulation at the m th time instant is $\tilde{x}_{i,m} \in \{\pm e^{j\varphi_{i,m}}\}$. This “phase scrambling” can improve the superimposed multi-user codeword distance [41], particularly in AWGN channels. For notational brevity, the symbol index m is dropped in the following.

The received signal is first processed by a MUD. An optimum MUD is to maximize the *a posteriori* probability (APP) of each bit, i.e.,

$$L_{M,i}(x_i|y_m) = \log \frac{\sum_{\mathbf{s} \in \mathcal{S}_{i,+1}} p(\mathbf{s}|y_m)}{\sum_{\mathbf{s} \in \mathcal{S}_{i,-1}} p(\mathbf{s}|y_m)} \quad (2)$$

where $\mathbf{s} = [x_1, x_2, \dots, x_N]$ denotes a symbol vector of all users, $\mathcal{S}_{i,+1}$ and $\mathcal{S}_{i,-1}$ with the cardinality 2^{N-1} are two sets containing the symbol vectors with $[s]_i = x_i = +1$ and $x_i = -1$, respectively. This requires a complexity of $O(M^N)$ where M denotes the number of constellation symbols per user. The exponentially increasing complexity with the number of users N prohibits its practical implementation. Therefore, a sub-

optimal soft interference cancellation (SoIC) based low complexity MUD was proposed in [18]. The sub-optimal MUD first cancels out other users’ signals; for instance with BPSK signaling, the i th user’s signal is estimated by the conditional mean estimate [45]

$$\hat{x}_i = E[x_i | L_{M,i}^A] = \tanh\left(\frac{L_{M,i}^A}{2}\right) \cdot e^{j\varphi_i} \quad (3)$$

based on, e.g., the feedback *extrinsic* knowledge from the single user channel decoder $L_{M,i}^A$. At the first iteration, the feedbacks from channel decoders are $L_{M,i}^A = 0$. The feedback procedure, i.e., message passing from channel decoder to the MUD, will be discussed later. For an arbitrary user j , the output of the MUD after the SoIC can be written as

$$\begin{aligned} y_j &= y - \sum_{i=1, i \neq j}^N \sqrt{P_i} h_i \hat{x}_i \\ &= \sqrt{P_j} h_j \tilde{x}_j + \sum_{i=1, i \neq j}^N \sqrt{P_i} h_i (\tilde{x}_i - \hat{x}_i) + n. \end{aligned} \quad (4)$$

Then, each user starts its single user detection and decoding in parallel based on the “clean observations” y_i . The (soft) demapper computes the log-likelihood-ratio (LLR) of each bit while treating the residual interference as noise. Assuming that the residual interference and noise is Gaussian-distributed and let $\sigma_{1,j}^2$ denote the residual interference power for j th user, an approxi-

mation of the true a posteriori LLR for BPSK can be computed according to

$$L_{M,j}^E = 4\sqrt{P_j} \frac{\text{Re} \{y_j \cdot h_j^* \cdot e^{-j\varphi_j}\}}{\sigma_{1,j}^2 + \sigma_n^2} \quad (5)$$

where the noise variance σ_n^2 , the random phase shifts φ_j and the channel coefficients h_j are assumed to be known to the receiver. The residual interference power after SoIC can be estimated by

$$\begin{aligned} \sigma_{1,j}^2 &= \mathbb{E} \left[\left| e^{-j\varphi_j} \sum_{i \neq j} \sqrt{P_i} h_i (\tilde{x}_i - \hat{x}_i) \right|^2 \right] \\ &= \sum_{i \neq j} P_i |h_i|^2 (1 - \mathbb{E} [\hat{x}_{i,m}^2]) \end{aligned} \quad (6)$$

where the expectation $\mathbb{E}[\cdot]$ is taken over m . We assume that the interference term is Gaussian distributed, which is approximately true provided that the number of users N is large and the transmitted symbols are independent among users (central limit theorem).

Subsequently, the LLRs are deinterleaved (denoted by $\tilde{L}_{M,j}^E = L_{R \leftarrow M,j}^A$ for the j th user which means the extrinsic message from MUD corresponds to the *a priori* knowledge of REP obtained by MUD) and sent to a repetition decoder with the rate of $R_r = \frac{1}{d_r}$. The extrinsic message of the k th information symbol of the repetition code is the summation of the LLRs of all repeated symbols, given by

$$L_{D,j,k}^A = L_{R \rightarrow D,j,k}^E = \sum_{m=kd_r}^{(k+1)d_r-1} \tilde{L}_{M,j,m}^E \quad (7)$$

where m means the m th symbol of the repetition-coded codeword and then it is forwarded to the LDPC decoder. Belief propagation (BP) decoding can be performed by iterating between variable nodes (VNs) and CNs of the LDPC code. The detailed decoding procedure will be discussed in Sec. III. Let $L_{D,j,k}^E = L_{R \leftarrow D,i,m}^A$ denote the extrinsic information about the k th symbol of an LDPC codeword, i.e., output of the LDPC decoder. The extrinsic message from the repetition decoder to the MUD can be written as

$$L_{R \rightarrow M,j,k}^E = \tilde{L}_{M,j,k}^A = L_{D,j,k}^E + \sum_{m=nd_r, m \neq k}^{(n+1)d_r-1} \tilde{L}_{M,j,m}^E. \quad (8)$$

Afterwards, the LLRs are again interleaved and remapped to soft symbols with (3) for the MUD processing with (4). In this way, multiple iterations can be carried out to reduce the MAI. It is worth noting that the receiver needs the knowledge of active users and their interleaver as well as phase scrambling for correct decoding.

Next, we discuss some key advantages of IDMA.

- 1) *Low complexity*: Comparing the computation of LLR in (5) and (2), the SoIC-based MUD is

quite simple and requires only few multiplications and additions for variance estimation, interference subtraction and LLR computation (see [19]). The complexity becomes $O(M \cdot N)$ and many computations can be carried out in parallel when compared to SIC. Particularly, when all the users apply an LDPC code with the same parity check \mathbf{H} -matrix, the coordination and code design among users can be dramatically reduced.

- 2) *Parallelizable computation*: The N single user channel decoders can independently perform their decoding at the same time. Since iterations between channel decoders and SoIC-MUD will be carried out, the number of inner iterations within the channel decoders can be kept very small. In fact, one iteration within the decoders suffices. In contrast, SIC requires a considerable large number of inner iteration within decoder for each user and often the operations are not parallelizable due to its sequential processing. Hence, the latency may be reduced in IDMA.
- 3) *Asynchronous transmission*: The SoIC-MUD principle in (4) is applicable to asynchronous transmissions. For instance, [46] shows that the performance of IDMA is insensitive to different user delays on the symbol-level. Without loss of generality, an asynchronous transmission of two users' signals is illustrated in Fig. 3. The delay between users is denoted by τ_d . Two or more consecutive codewords shall be decoded within one common detection window and interference cancellation can be performed within the window decoder principle in [47].

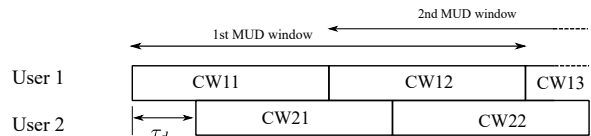


Fig. 3. The iterative receiver processing of an asynchronous transmission of two users' signals in IDMA; without loss of generality, the delay τ_d between both users satisfies $0 < \tau_d < \tau_{cw}/2$ where τ_{cw} is the time duration of one codeword.

III. MULTIUSER EXIT ANALYSIS

In order to optimize the LDPC degree profile, we elaborate on the EXIT-chart approach in the context of IDMA by separately and/or jointly considering the components of the multistage iterative receiver (MUD, repetition decoder and LDPC decoder). For this, we illustrate the graph representation of the BP based receiver in Fig. 4. Furthermore, since we consider a system with a large number of users, the messages being exchanged over the graph (LLRs) can be assumed to be Gaussian distributed. We consider AWGN channels in the EXIT analysis in the following, i.e., $h_{i,m} = 1, \forall i, m$.

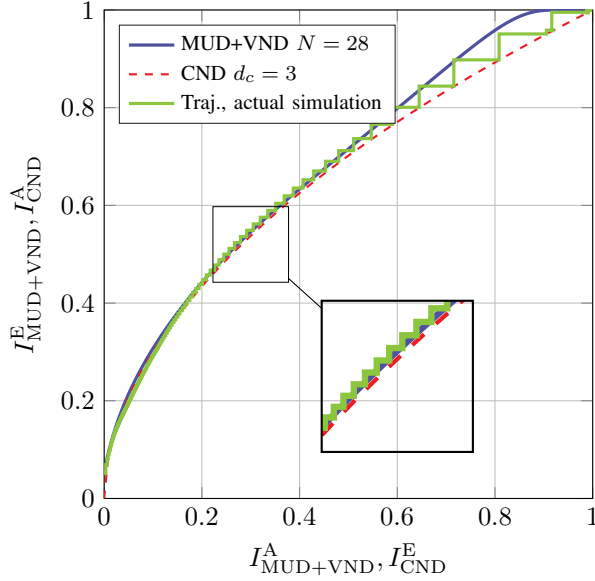


Fig. 5. EXIT-chart along with simulated trajectories of MUD and REP in an “uncoded” IDMA system with $N = 32$ users and $\gamma_{s,\text{mu}} = 40$ dB; all users have the same power $P_i = \frac{1}{N}$; the MAC system is mainly interference-limited (see. Sec. IV-A) and the repetition code is particularly effective in this operation regime (compare to Fig. 7).

obtained by numerical simulations match very well with the EXIT-curve predictions. Small deviations are still present in the high a priori knowledge region, i.e., large $J(\mu_{R \rightarrow M})$, due to the GA.

C. VN and CN

The message exchange and update between VND and CN decoder (CND) is well known [24]. For the sake of completeness, we review and incorporate it into IDMA systems. Denote λ_i and ρ_j as the fraction of edges connected to VNs and CNs with degrees i and j , respectively. The message means $\mu_{V \rightarrow C}^i$ and $\mu_{C \rightarrow V}^j$, i.e., the mean of message from CN (or VN) to VN (or CN) of degree i (or j) respectively, are given by

$$\mu_{V \rightarrow C}^i = \mu_{R \rightarrow V} + (i-1) \cdot \sum_{j=2}^{c_{\max}} \rho_j \mu_{C \rightarrow V}^j$$

where c_{\max} denotes the maximum degree of CNs, and

$$\mu_{C \rightarrow V}^j = \phi^{-1} \left(1 - \left(1 - \sum_{i=2}^{v_{\max}} \lambda_i \phi(\mu_{V \rightarrow C}^i) \right)^{j-1} \right)$$

where v_{\max} denotes the maximum degree of VNs and the channel observation of the VND is now provided by the REP. Note that the $\phi(\mu)$ function given in (10) in this paper is equivalent to that in [49, Def. 1] by means of change of variables. Furthermore, we consider *check-regular* LDPC codes, i.e., $\rho_j = 1$ for a given $d_c = j$. The

VND also passes a message to the connected repetition node, given by

$$\mu_{V \rightarrow R}^i = i \cdot \sum_{j=2}^{c_{\max}} \rho_j \mu_{C \rightarrow V}^j.$$

IV. UNIVERSAL CODE DESIGN

The detection and decoding of signals in the MAC is challenging not only due to the noise but also due to the MAI. The code design for the MAC therefore depends also on the relation between the MAI and the noise. We briefly discuss the code design for different operation regimes of a MAC in the following and then present a flexible code design for a dynamic MAC system with varying number of users.

A. Operation Regime

In a multi-user transmission, the achievable sum-rate is determined by the multi-user SNR given by

$$\gamma_{s,\text{mu}} = \frac{\sum_{i=1}^N P_i \cdot \mathbb{E}[|h_i|^2]}{\sigma_n^2}$$

and the ultimate achievable rate of each user is determined by the single-user SNR, e.g., for the i th user we have

$$\gamma_{s,\text{su}}(i) = \frac{P_i \cdot \mathbb{E}[|h_i|^2]}{\sigma_n^2}.$$

However, this single-user SNR is only attainable when all other users' signals are perfectly decoded and canceled out. In the iterative detection and decoding procedure, the performance is limited by both noise and MAI, i.e.,

$$\frac{P_i \cdot \mathbb{E}[|h_i|^2]}{\underbrace{\sum_{j=1, j \neq i}^N P_j \cdot \mathbb{E}[|h_j|^2] + \sigma_n^2}_{\sigma_{I,i}^2}} \leq \gamma_{s,\text{su}}(i) \leq \frac{P_i \cdot \mathbb{E}[|h_i|^2]}{\sigma_n^2}.$$

Depending on the noise variance and MAI, we can distinguish three regimes of operation:

- 1) The noise-limited case, with the noise power dominating, i.e., $\sigma_n^2 \gg \sigma_{I,i}^2$. Single user code design is sufficient since the effect of removing the MAI is marginal.
- 2) The MAI-limited case, with MAI dominating, i.e., $\sigma_{I,i}^2 \gg \sigma_n^2$. Orthogonal approaches and/or repetition coding are sufficient. We will see an example of this regime of operation in the following section.
- 3) The MAI and noise-limited case, with $\sigma_{I,i}^2 \approx \sigma_n^2$. This case is quite challenging and of most practical interest. This paper mainly focuses on this case.

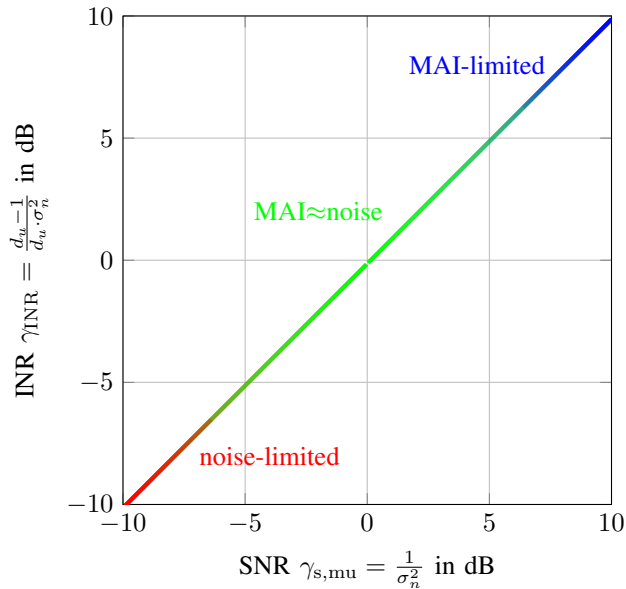


Fig. 6. Illustration of the three operation regimes, i.e., noise-limited, MAI-limited, MAI and noise-limited; equal user power is assumed, i.e., $P_1 = P_2 = \dots = P_N = \frac{1}{N}$. For example, $\sigma_{I,i}^2 \approx \sigma_n^2$ may be assumed when the ratio $\frac{\sigma_{I,i}^2}{\sigma_n^2}$ is within ± 3 dB.

Fig. 6 illustrates the three regimes of operation assuming equal transmit power per user. The interference-to-noise ratio (INR) case can then be written as

$$\gamma_{\text{INR}} = \frac{N-1}{N} \cdot \gamma_{s,\text{mu}}.$$

B. LDPC Code Only

The LDPC degree profile, i.e., the coefficients λ_i and ρ_j , can be optimized to match (curve fitting) the EXIT-curve of the inner SoIC-MUD. The optimization approach is summarized in Algorithm 1. The repetition code is excluded at first in this subsection, i.e., $d_r = 1$ and all redundancy is devoted to the LDPC code. In this case, the MUD, repetition and VND nodes can be merged into one effective MUD-VND node, and message passing is performed solely between CND and MUD-VND nodes. As shown in Appendix A, the stability condition in (21) is derived. The LDPC code shall be optimized and used to mitigate the MAI and noise disturbance. Note that the initial SINR (no iteration) can be very small. For instance, the SINRs are -18 dB and -14.7 dB for $\gamma_{s,\text{mu}} = 0$ dB and 40 dB (both cases with $N = 32$ users), respectively.

In Fig. 7, we show the EXIT-chart of the optimized LDPC code of rate $R_c = 0.1068$ at $\gamma_{s,\text{mu}} = 40$ dB and $N = 32$. We limit the maximum VN and CN degrees to $v_{\text{max}} = 320$ and $c_{\text{max}} = 64$ to enable feasible finite

Algorithm 1 LDPC code design based on EXIT-charts with and without repetition code.

Input: Number of users N , maximum VN degree v_{max} , maximum CN degree c_{max} , maximum repetition factor r_{max} , noise variance σ_n^2

Output: Optimal VN degree distribution λ_{opt} , optimal VN degree distribution ρ_{opt} , optimal repetition factor $d_{r,\text{opt}}$, maximal code-rate R_{max}

for $d_r = 1$ to r_{max}

for $d_c = 2$ to c_{max}

Solve LP:

$$\max_{\lambda_{\text{opt}}} \sum_{i=2}^{v_{\text{max}}} \frac{\lambda_i}{i}$$

$$\text{s.t. } \lambda_i \geq 0$$

$$\sum_{i=2}^{v_{\text{max}}} \lambda_i = 1$$

$$1 - \sum_{i=2}^{v_{\text{max}}} \lambda_i \phi(d_r \cdot \bar{\mu}_{M \rightarrow R}(i \cdot \mu) + (i-1) \cdot \mu)$$

$$> d_c^{-1} \sqrt{1 - \phi(\mu)} \quad (20)$$

$$\lambda_2 \leq \frac{e^{\frac{1}{N\sigma_n^2}}}{d_c - 1} \quad (21)$$

$$\text{Compute } R = \frac{1}{d_r} \cdot \left(1 - \frac{1}{d_c \sum_{i=2}^{v_{\text{max}}} \frac{\lambda_i}{i}} \right)$$

end

end

Select the maximum R_{max} and output the corresponding $d_{r,\text{opt}}$, λ_{opt} and ρ_{opt} .

length code constructions². In the simulation, random but user-specific interleavers are used and the LDPC code-word length is set to $L_{\text{CW}} = 10^4$. Throughout the paper, the parity check matrices \mathbf{H} are randomly generated according to the optimized LDPC degree profile, and then the matrix with the largest average girth is selected for numerical simulation.

It turns out that convergence is achieved with $N = 28$ users when fixing the multi-user SNR $\gamma_{s,\text{mu}}$ to 40 dB. We treat the SoIC-MUD nodes and the VND of the LDPC as one component, and the CND as another component. The analytical EXIT-functions are depicted by the solid blue and dashed red curves, respectively. For each iteration, the mutual information of the exchanged messages between the two components is simulated. The average decoding trajectory (denoted by green staircase, obtained from simulation) is shown in Fig. 7 for 171 iterations. It can be seen that the trajectory matches quite

²It turns out that not all degrees, particularly the high degrees, are needed.

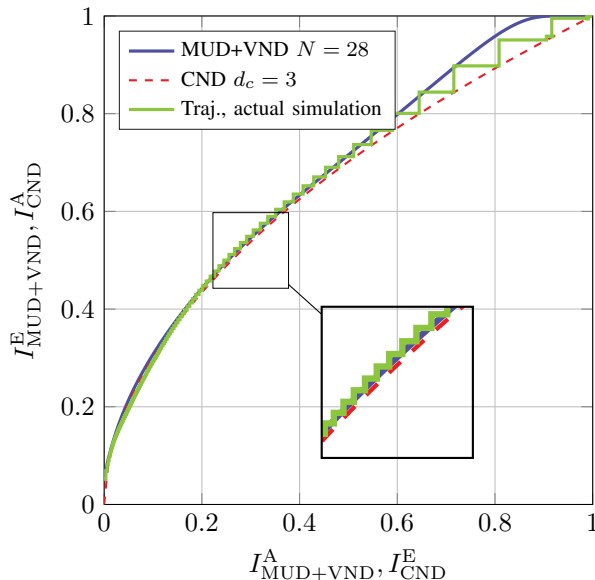


Fig. 7. EXIT-chart of an optimized LDPC code with Algorithm 1 at SNR of $\gamma_{s,\text{mu}} = 40$ dB with $N = 28$ and $R_c = 0.1068$; the system operates in the MAI-limited regime; the achievable rate with optimized LDPC code is smaller than that with simple a repetition code (compare with Fig. 5).

well with the analytical EXIT-functions, which verifies the viability of the algorithm.

The optimized LDPC code at such high SNR is not as efficient as the simple repetition code both in terms of decoding complexity and achievable sum-rate. In the repetition-coded system, a $R_r = 1/9$ repetition code is able to support 32 users and practically achieves error-free decoding in 20 iterations (comparing Fig. 5), leading to the sum-rate of $R_{\text{sum}}^{\text{REP}} = NR_r = 3.56$ bpcu. With the optimized LDPC code, the achievable rate of $R_{\text{sum}}^{\text{LDPC}} = NR_c = 2.99$ bpcu is achieved with 171 iterations. At such high SNR $\gamma_{s,\text{mu}} = 40$ dB, the performance is mainly interference-limited. Interestingly, the required minimal repetition code rate is $\frac{1}{9}$ while a spreading factor of 16 would be necessary in an orthogonal CDMA scheme. This indicates that repetition codes are very efficient for interference cancellation. In a more realistic SNR region, the noise sets the upper limit on the MUD, i.e., $I_E = J\left(\frac{1}{N\sigma_n^2}\right)$. Therefore, an LDPC code is further required to mitigate the noise disturbance, as described next.

In Fig. 9, the BER of the optimized LDPC code at the target sum-rate of $R_{\text{sum}} = N\frac{R_c}{d_r} = 1$ bpcu is shown. The interleaver depth is set to $d_r L_{\text{CW}}$ bits in the simulation to mitigate short cycles due to the superposition of multiple users. It turns out that the performance depends, to a great extent, on the number of users N . In the simulation, we set the number of users to $N = 30$ although the code is optimized for $N = 32$; this “slack”

is to account for a possibly small girth of the parity check matrix and any other finite length effects that would slow down convergence. The corresponding GMAC capacity is achieved at -0.1 dB, and the optimized code is more than 6 dB away from the GMAC capacity. The reasons are manifold; firstly, it is well known that LDPC code design does not yield satisfactory performance at low code rates [25]; secondly, the BP-graph is rather dense so that convergence is compromised. We remark that the performance can be improved by increasing the interleaver depth and/or constructing \mathbf{H} matrices using more sophisticated design methods such as progressive edge growth (PEG) [50] and methods in [51].

C. Repetition code and LDPC

The repetition code seems to be an effective means for supporting interference cancellation. Thus, we extend the LDPC degree profile optimization to a serially concatenated repetition code with $d_r > 1$. The procedure for the optimization of the degree profile involving a repetition code is summarized in Algorithm 1. If a target code rate R_c is required, the Algorithm 1 can be recursively applied for different values of the noise variance σ_n^2 (e.g., bisection method depending on the code-rate output of the algorithm). Hereby, the MUD, repetition and VND nodes are merged into one effective MUD-REP-VND node. Within this node, a sufficient number of iterations is carried out so that the messages between MUD and repetition node have converged. The converged message mean, denoted by $\bar{\mu}_{M \rightarrow R}(i \cdot \mu)$, depends on the incoming message from the connected VND $\mu_{V \rightarrow R}^i = i \cdot \mu$ and can be obtained by solving (18).

In Fig. 8, we present the $\frac{E_b}{N_0}$ -gap to the Shannon limit of the joint repetition and LDPC code optimization for various repetition factors d_r and a few target sum-rates, where the gap is calculated as

$$\Delta\gamma = \frac{\zeta_t}{2^{R_{\text{sum}}} - 1}$$

where ζ_t denotes the decoding threshold (required SNR) and R_{sum} denotes the achieved sum rate of all users. As can be observed, there exists an optimum repetition code rate $\frac{1}{d_r}$ for the outer LDPC code rate R_c which maximizes the spectral efficiency. The optimum repetition factor d_r is marked in Fig. 8. This also indicates that repetition codes are efficient for interference cancellation, since it is well known that repetition codes have no coding gain in the single user case. We note that the SoIC-MUD based on GA is sub-optimal for the finite modulation. The loss incurred by the sub-optimality becomes significant when the SNR increases. Thus, the $\frac{E_b}{N_0}$ -gap is larger when the target sum-rate increases.

We select the target sum rate of $R_{\text{sum}} = 1$ bpcu whose GMAC capacity is achieved at $\frac{E_b}{N_0} = \gamma_{s,\text{mu}} = 0$ dB. In

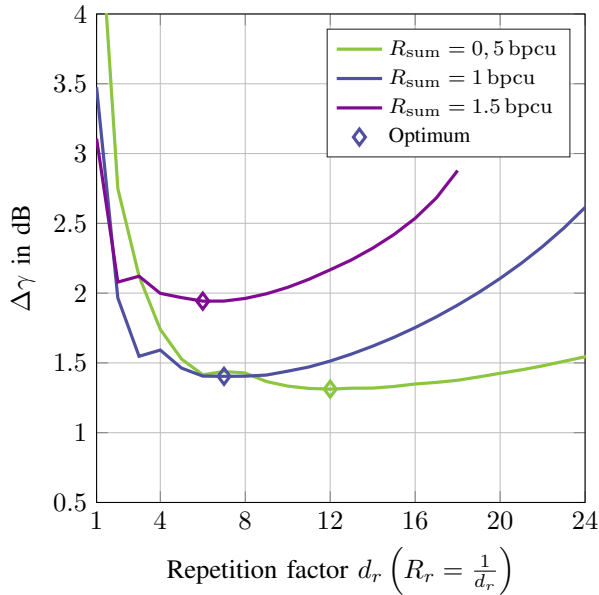


Fig. 8. Impact of the repetition code on the BP-threshold of the LDPC code design and the (BP) gap-to-capacity $\Delta\gamma$ with $N = 32$ users.

this case, the MAI and the noise have approximately the same power such that the interference cancellation and error correction are of comparable importance. The INR

Table I
LDPC PARAMETERS

$N = 32$ and $R_{\text{sum}} = N \frac{R_c}{d_r} = 1$ bpcu	
$d_r = 2$	$d_r = 4$
$R_c = 0.0625$	$R_c = 0.125$
$R_{\text{tot}} = 0.03125$	$R_{\text{tot}} = 0.03125$
$d_c = 3, \rho_3 = 1$	$d_c = 3, \rho_3 = 1$
$\lambda_2 = 0.5252$	$\lambda_2 = 0.5231$
$\lambda_3 = 0.2112$	$\lambda_3 = 0.3187$
$\lambda_9 = 0.1030$	$\lambda_{12} = 0.1582$
$\lambda_{10} = 0.0915$	
$\lambda_{35} = 0.0587$	
$\lambda_{36} = 0.0104$	
$d_r = 6$	$d_r = 8$
$R_c = 0.1875$	$R_c = 0.25$
$R_{\text{tot}} = 0.03125$	$R_{\text{tot}} = 0.03125$
$d_c = 4, \rho_3 = 1$	$d_c = 5, \rho_3 = 1$
$\lambda_2 = 0.3480$	$\lambda_2 = 0.2610$
$\lambda_3 = 0.3450$	$\lambda_3 = 0.3505$
$\lambda_{15} = 0.1829$	$\lambda_{16} = 0.2526$
$\lambda_{16} = 0.0939$	$\lambda_{17} = 0.0361$
$\lambda_{49} = 0.0302$	$\lambda_{70} = 0.0778$
	$\lambda_{71} = 0.0220$

can be calculated to $\gamma_{\text{INR}} = -0.1379$ dB with $N = 32$. The optimized LDPC code parameters³ are given in Tab. I.

³The parity check \mathbf{H} -matrices used for the simulation in this paper can be found in [52]

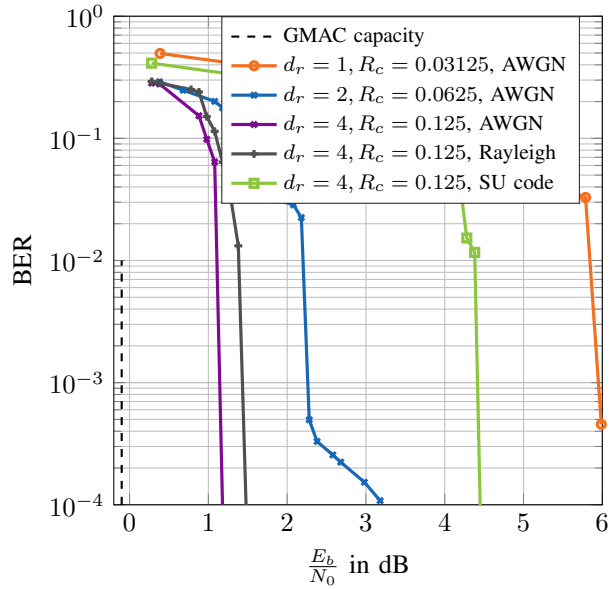


Fig. 9. BER comparison for $R_{\text{sum}} = 0.9375$ bpcu with $N = 30$ users and the repetition factors $d_r = 1, 2$ and 4 ; the overall per-user code-rate is $R_{\text{tot}} = \frac{R_c}{d_r} = 0.03125$; the codes are optimized for $N = 32$ users except for the single-user reference (“SU code”), denoted by the green curve.

Fig. 9 shows the BER for different repetition factors d_r . The optimized code with $d_r = 4$ achieves the BER of 10^{-4} at the $\frac{E_b}{N_0}$ of 1.18 dB, which is only 1.28 dB away from the GMAC capacity (the corresponding $\frac{E_b}{N_0}$ GMAC limit is -0.1 dB). The performance gain through inclusion of a repetition code is obvious. Further increase of the repetition factor does not offer significant gains (not shown). Moreover, the Rayleigh fading channel is considered for $d_r = 4$. Only 0.2 dB loss is incurred compared to the AWGN channel. This is due to the multi-user diversity in the multi-access fading channels [8] and the low-rate per user. To validate the matching gain of the multi-user code design, i.e., the performance gain of a dedicated LDPC code optimization for a multi-user setup compared to an LDPC code optimized for a single-user setup, we further simulate the performance of a single-user code of rate $R_c = 0.125$ which is optimized for the single-user (SU) AWGN channel. To support $N = 30$ users in IDMA, the optimized SU code is serially concatenated with the REP code ($d_r = 4$), yielding a matching gain of more than 3 dB.

D. Repetition as User-load Equalizer

The degree profile optimization and the finite-length code construction of the LDPC code is computationally quite expensive particularly if the repetition code is serially concatenated and/or more sophisticated optimizations are considered (e.g., “full” density evolution and/or irregular CNs). When the number of users varies

in a system, usually, the code would have to be re-optimized to achieve closer to MAC capacity, or several pre-optimized LDPC codes have to be stored for each possible scenario (e.g., amount of users, transmit power distribution, channel condition). This limits the flexibility and practical usability of multiple access schemes that are based on variants of superposition coding, like IDMA. In the following we show how this issue can be mitigated, working close to capacity for any user load using the *same* LDPC parity check matrix \mathbf{H} by just adapting the repetition code rate $R_r = \frac{1}{d_r}$.

Considering the LDPC code (the same for all users), we observe that the “channel observation” of the VN is provided by the MUD+REP detector and its message mean is given by $\mu_{R \rightarrow V}$. Allowing a sufficient number of iterations between the repetition node and the MUD, we obtain the “channel input” to the VN of the LDPC code by combining (17) and (18) as

$$\mu_{R \rightarrow V} = \frac{d_r}{N} \frac{4}{\sigma_n^2 + (1 - \frac{1}{N}) \phi((d_r - 1) \bar{\mu}_{M \rightarrow R} + \mu_{V \rightarrow R})}.$$

This “channel input” to the LDPC decoder depends on *three* system parameters, i.e., N , d_r and σ_n^2 . Note that it also depends on the feedback information from the channel decoder $\mu_{V \rightarrow R}$, however, we do not consider it as system parameter. In other words, the “channel input” is characterized by a *three dimensional* function, i.e., $\mu_{R \rightarrow V}(N, d_r, \sigma_n^2)$. We prove that the dimensionality can be further reduced to $\mu_{R \rightarrow V}(\frac{d_r}{N}, \sigma_n^2)$. Thus, we introduce a *repetition to user load ratio* (RUR) γ_{RUR} which is defined by

$$\gamma_{RUR} = \frac{d_r}{N}.$$

According to the proof in Appendix B, we show that

$$\lim_{\substack{N \rightarrow \infty \\ \frac{d_r}{N} \rightarrow \gamma_{RUR}}} \mu_{R \rightarrow V}(N, d_r, \sigma_n^2) = \mu_{R \rightarrow V}(\gamma_{RUR}, \sigma_n^2). \quad (22)$$

Empirically, the approximation of the “channel input” to the LDPC decoder, expressed as

$$\mu_{R \rightarrow V}(N, d_r, \sigma_n^2) \approx \mu_{R \rightarrow V}(\gamma_{RUR}, \sigma_n^2), \quad (23)$$

is quite accurate also for small number of users through the EXIT analysis using (18) (EXIT curves not shown in the paper, however, BER simulation results are shown in Fig. 11).

This feature is particularly important in terms of adaptiveness to the user load N . For instance, if the number of active users decreases or increases, the LDPC decoder “sees” a better or worse channel, respectively, which drifts the system operating point away from capacity⁴ or the system collapses⁵. If the approximation in (23) holds,

⁴When the channel becomes better, the code rate of the LDPC code can be higher.

⁵The optimized LDPC code at certain SNR can not operate when the real SNR becomes smaller.

we may only need to vary the d_r accordingly to maintain the constant RUR γ_{RUR} so that the “channel input” to the LDPC decoder remains unchanged and subsequently the coding part is decoupled from the multi-user front-end via the repetition code component.

Fig. 10 shows the gap-to-GMAC capacity where the LDPC code of rate $R_c = 0.0975$ (optimized for $N = 32$, $d_r = 4$ and $\gamma_{s,mu} = 0$ dB) is kept invariant. The number of users N and the repetition factor d_r are varied. Density evolution based on GA is used to estimate the

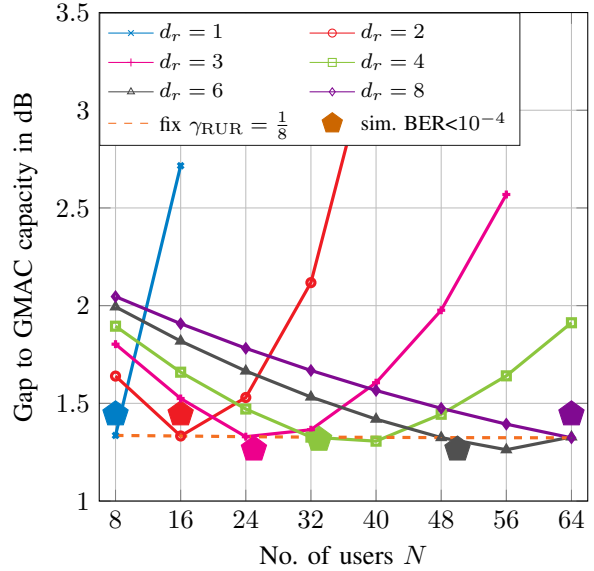


Fig. 10. GA-density evolution-based $\frac{E_b}{N_0}$ -gap to GMAC capacity for varying γ_{RUR} with the **same** LDPC code optimized for $d_r = 4$, $N = 32$ users and $\gamma_{s,mu} = 0$ dB; the dashed line depicts the operation points with adaptive repetition factor according to the user load by fixing the RUR to a constant $\gamma_{RUR} = \frac{1}{8}$; pentagons denote actual simulation results at the BER of 10^{-4} ; Note that the **same** \mathbf{H} -matrix is used for all simulations.

decoding threshold for each combination of d_r and N . Obviously, the spectral efficiency is quite invariant if the RUR $\gamma_{RUR} = \frac{1}{8}$ is kept constant. The BER simulation results are also included as pentagons with corresponding colors in Fig. 10, where the required SNR is obtained at the BER of 10^{-4} . We note that this adjustment of the repetition code does not incur any significant loss of spectral efficiency and can be easily reconfigured at the transmitter and receiver due to its simple structure and decoding procedure. Furthermore, the simulated BERs at the multi user SNR $\gamma_{s,mu} = 0$ dB are shown in Fig. 11 for $1 \leq d_r \leq 8$ and various N . The results consolidate our analytical and empirical expression in (22) and (23). It also suggest that the designed LDPC code for specific parameters can be easily generalized and reused in systems with arbitrarily varying user load by simply adjusting the repetition factor.

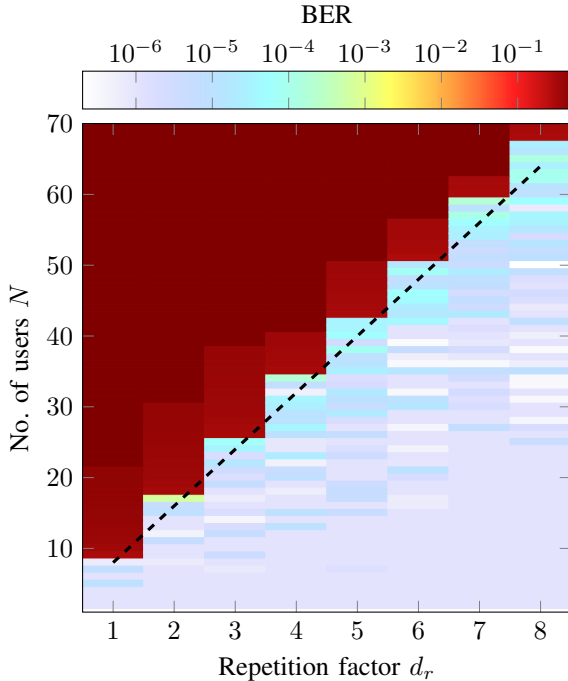


Fig. 11. BER comparison of IDMA system with different repetition factor d_r and number of users N ; the LDPC code optimized for $d_r = 4$, $N = 32$ and $\gamma_{s,\text{mu}} = 0$ dB remains fixed; the dashed black curve denotes $\gamma_{\text{RUR}} = \frac{1}{8}$.

V. BEYOND EQUAL POWER AND RATE

Different users' signals arrive at the base-station (BS) with different power levels since the path loss between the BS and individual users may be quite different. This fact indicates that the user rate shall be adapted to its power level. We assume that each user transmits at full power for higher data rates and propose two approaches in the following to allow for multi-rate transmission, yet using the same channel code that is optimized for the equal-power case.

- 1) *Layer aggregation*. The higher power users may divide their signals into several *data layers* or “*virtual users*”, each with a smaller power and thus, the user with weakest power can only transmit one data layer. This approach is straightforward, thus not further discussed.
- 2) *Repetition code adaptation (RCA)*. The serially concatenated repetition code can be further applied as a “power equalizer” in unequal receive (or transmit) power cases, or, more precisely, as an “energy equalizer”. Users with higher power can reduce the repetition factor d_r and users with lower power shall increase the repetition factor. Let P_i and $d_{r,i}$ denote the signal power and repetition factor of the user i , we show that the “channel

input” to the i th LDPC decoder can be written as

$$\mu_{R \rightarrow v} = \frac{4\gamma_{\text{RCA}}}{\sigma_n^2 + \phi(\kappa(\gamma_{\text{RCA}}))} \quad (24)$$

in the asymptotic case of $P_i \rightarrow 0$ while $P_i \cdot d_{r,i} \rightarrow \gamma_{\text{RCA}} = \text{const.}$, where $\kappa(\gamma_{\text{RCA}})$ is a constant depending on the feedback from the channel decoders and the value of γ_{RCA} . A detailed derivation is given in Appendix C.

For simplicity of numerical simulation, we consider the following unequal power IDMA system

$$y = \sqrt{P_{\text{st}}} \sum_{i=1}^{N/2} \tilde{x}_i + \sqrt{P_{\text{wk}}} \sum_{j=\frac{N}{2}+1}^N \tilde{x}_j + n$$

where half of the users $\frac{N}{2}$ (without loss of generality, N is assumed to be even) exhibit a higher power than the other half number of users, i.e., $P_{\text{st}} > P_{\text{wk}}$. The total power is normalized to one, that is,

$$P_{\text{st}} + P_{\text{wk}} = \frac{2}{N}$$

and we define a new quantity of “power asymmetry” as $P_A = \frac{P_{\text{st}}}{P_{\text{wk}}}$. The repetition code adaptation rule is given by

$$\frac{d_{r,\text{wk}}}{d_{r,\text{st}}} = P_A$$

$$\frac{1}{d_{r,\text{wk}}} + \frac{1}{d_{r,\text{st}}} = \frac{2}{d_r}$$

where $d_{r,\text{wk}}$ and $d_{r,\text{st}}$ denote the new repetition factor for the strong and weak users, respectively. Notice that if $d_{r,\text{wk}}$ and $d_{r,\text{st}}$ are not integer-valued, irregular or quasi-regular repetition codes with the corresponding average repetition factors shall be applied.

In Fig. 12, we show the BER performance of an unequal-power IDMA system with the power asymmetry between strong users and weak users of $P_A = 3$ dB. The LDPC code remains unchanged ($R_c = 0.125$ and $d_r = 4$). As the LDPC code is optimized for the equal power case, the average performance becomes worse since the weak users require higher SNRs. If the RCA is applied where the strong users employ a repetition factor of $d_{r,\text{st}} = 3$ and the weak users employ the new repetition factor of $d_{r,\text{wk}} = 6$ instead of $d_r = 4$, then a similar performance can be achieved compared to the equal power case, as the adapted repetition rate acts as a “power equalizer”. The extension to other cases of asymmetric power distribution is straightforward.

VI. CONCLUSION

We have proposed a flexible and simple coding scheme to achieve near-capacity performance in a dynamic multiple access channel (MAC) system with both a varying number of users as well as varying transmit (or receive) power levels. In particular, a joint optimization

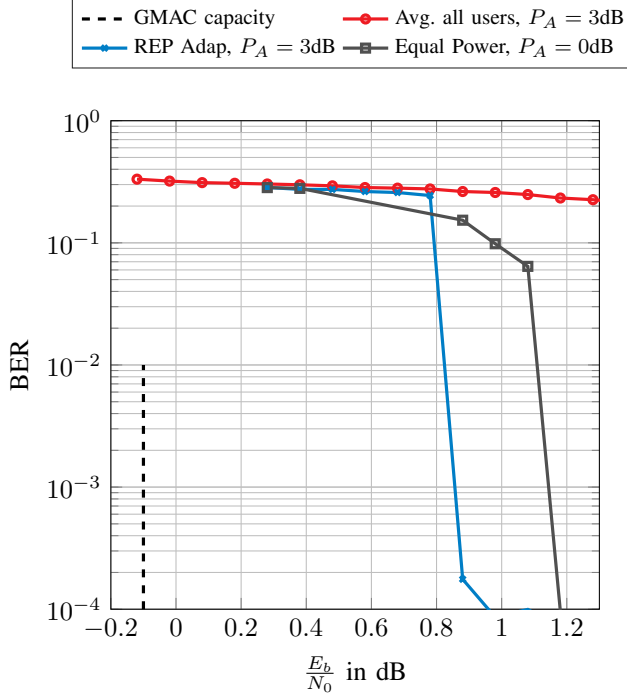


Fig. 12. BER comparison of unequal-power IDMA system with the power asymmetry of $P_A = 3$ dB; the LDPC code is optimized for the equal-power case with $d_r = 4$, $N = 32$.

of serially concatenated LDPC and repetition code is considered in a low-complexity IDMA system. We show that near-capacity performance can be maintained with the same LDPC code regardless of the number of users and signal power levels. This universality of the proposed scheme is made possible by the repetition code acting as both an interference equalizer as well as power equalizer, which is of particularly practical interest. The same LDPC parity check matrix allows to cover a remarkably wide range of scenarios with respect to number of users and transmit powers, making this highly flexible and simple NOMA scheme an attractive candidate for future wireless communication systems.

APPENDIX A PROOF OF (21)

The stability condition requires that the message μ approaches infinity as the number of iterations goes to infinity. Assume that a very large μ_l is reached after a finite number of iterations and let $\tilde{\mu}_l$ denote

$$\tilde{\mu}_l = \mu_l + \frac{4}{N\sigma_n^2 + (N-1) \cdot \phi(2 \cdot \mu_l)}.$$

The left term of (21) is lower-bounded with Taylor-series by

$$\begin{aligned} \text{left term of (21)} &\geq 1 - \lambda_2 \phi'(\tilde{\mu}_l) \cdot \Delta\mu \\ &\quad + \frac{8\lambda_2 \phi'(2\mu_l)}{(N\sigma_n^2 + (N-1) \cdot \phi(2 \cdot \mu_l))^2} \Delta\mu \end{aligned}$$

and when $\mu_l \rightarrow \infty$, we have $\tilde{\mu}_l \rightarrow \mu_l + \frac{4}{N\sigma_n^2}$ and the left term can be written as

$$1 - \lim_{\mu_l \rightarrow \infty} \lambda_2 \phi' \left(\underbrace{\mu_l + \frac{4}{N\sigma_n^2}}_{\mu_{\text{ch}}} \right) \cdot \Delta\mu.$$

Similarly, the right term of (21) is approximated by

$$1 - \frac{1}{d_c - 1} \lim_{\mu_l \rightarrow \infty} \phi'(\mu_l) \cdot \Delta\mu.$$

Therefore, we obtain

$$\begin{aligned} \lambda_2 &\leq \frac{1}{d_c - 1} \cdot \lim_{\mu_l \rightarrow \infty} \frac{\phi'(\mu_l)}{\phi'(\mu_l + \mu_{\text{ch}})} \\ &= \frac{e^{\frac{\mu_{\text{ch}}}{4}}}{d_c - 1} \end{aligned}$$

We note that $\phi(\mu) \approx \sqrt{\frac{\pi}{\mu}} e^{-\frac{\mu}{4}}$ is a tight approximation when μ is large.

APPENDIX B PROOF OF (22)

It is sufficient to show that the extrinsic output of the MUD+REP remains the same for an arbitrary a priori information from the LDPC decoder, provided that the RUR is constant, i.e., $\gamma_{\text{RUR}} = \text{const}$. Let $I_{R \leftarrow D}^A$ denote the a priori information from the LDPC decoder to the repetition decoder. The extrinsic message from repetition code to the MUD can be written as

$$I_{R \rightarrow M}^E = J \left((d_r - 1) \cdot J^{-1}(I_{MUD}^E) + J^{-1}(I_{R \leftarrow D}^A) \right)$$

where I_{MUD}^E denotes the extrinsic message from MUD to REP, given in (19) with $I_{MUD}^E = I_{R \rightarrow M}^E$. After sufficient iterations between MUD and REP, the intersection of EXIT functions of MUD and REP can be written as

$$\begin{aligned} &J \left(\frac{J^{-1}(I_{R \rightarrow M}^E) - J^{-1}(I_{R \leftarrow D}^A)}{d_r - 1} \right) = \\ &J \left(\frac{4}{N\sigma_n^2 + (N-1) \cdot \phi(J^{-1}(I_{R \rightarrow M}^E))} \right). \end{aligned}$$

With some mathematical manipulation, we obtain

$$\kappa \sigma_n^2 + \left(1 - \frac{1}{N} \right) \phi(\kappa) \cdot (\kappa - \nu_D) = \nu_D \sigma_n^2 + 4 \frac{d_r - 1}{N} \quad (25)$$

where $\kappa = J^{-1}(I_{R \rightarrow M}^E)$ denotes the converged message between MUD and REP for a given a priori information from LDPC decoder $\nu_D = J^{-1}(I_{R \leftarrow D}^A)$.

Let

$$N \rightarrow \infty \text{ while } \frac{d_r}{N} \rightarrow \gamma_{\text{RUR}} = \text{const.} \quad (26)$$

Thereby, (25) can be written as

$$\kappa \sigma_n^2 + \phi(\kappa) \cdot (\kappa - \nu_D) = \nu_D \sigma_n^2 + 4\gamma_{\text{RUR}}.$$

Clearly, the solution of $\kappa(\gamma_{\text{RUR}})$ to the above equation merely depends on γ_{RUR} , σ_n^2 and ν_D . Therefore, the message from REP to LDPC decoder for next iteration is given by

$$\mu_{R \rightarrow V} = \frac{4d_r}{N\sigma_n^2 + (N-1) \cdot \phi(\kappa)} \stackrel{(26)}{=} \gamma_{\text{RUR}} \frac{4}{\sigma_n^2 + \phi(\kappa)}.$$

APPENDIX C PROOF OF (24)

We first assume that the messages passed from REP to MUD are of the same mean value among all users, denoted by $\mu_{R \rightarrow M, i} = J^{-1}(I_{R \rightarrow M}^E)$, $\forall i$. Following the same approach in Appendix B, the intersection of EXIT functions of MUD and REP for the i th user can be written as

$$J \left(\frac{J^{-1}(I_{R \rightarrow M}^E) - J^{-1}(I_{R \leftarrow D}^A)}{d_{r,i} - 1} \right) = J \left(\frac{4P_i}{\sigma_n^2 + \sum_{j=1, j \neq i}^N P_j \cdot \phi(J^{-1}(I_{R \rightarrow M}^E))} \right).$$

With some mathematical manipulation and let the total power be normalized to 1, i.e., $\sum_{i=1}^N P_i = 1$, we obtain

$$\kappa \sigma_n^2 + (1 - P_i) \phi(\kappa) \cdot (\kappa - \nu_D) = \nu_D \sigma_n^2 + 4P_i (d_{r,i} - 1) \quad (27)$$

where $\kappa = J^{-1}(I_{R \rightarrow M}^E)$ denotes the converged message between MUD and REP for a given a priori information from LDPC decoder $\nu_D = J^{-1}(I_{R \leftarrow D}^A)$. Considering the following asymptotic

$$P_i \rightarrow 0, P_i d_{r,i} \rightarrow \gamma_{\text{RCA}} = \text{const.}, \forall i \quad (28)$$

we can re-write (27) as

$$\kappa \sigma_n^2 + \phi(\kappa) \cdot (\kappa - \nu_D) = \nu_D \sigma_n^2 + 4\gamma_{\text{RCA}}. \quad (29)$$

Clearly, the solution of $\kappa(\gamma_{\text{RCA}})$ to the above equation merely depends on γ_{RCA} . Therefore, the message from REP to LDPC decoder for next iteration is given by

$$\mu_{R \rightarrow V} = \frac{4P_i d_{r,i}}{\sigma_n^2 + (1 - P_i) \cdot \phi(\kappa)} \stackrel{(28)}{=} \gamma_{\text{RCA}} \frac{4}{\sigma_n^2 + \phi(\kappa)}. \quad (30)$$

Next, we prove that the messages passed from REP to MUD are of the same mean value among all users, e.g., $\mu_{R \rightarrow M, i} = J^{-1}(I_{R \rightarrow M}^E)$, $\forall i$. According to (16),

the message mean from REP to MUD of user i can be written as

$$\mu_{R \rightarrow M, i} = (d_{r,i} - 1) \frac{4P_i}{\sigma_n^2 + (1 - P_i) \cdot \phi(\kappa)} + \nu_D \quad (31)$$

$$\stackrel{(28)}{=} \mu_{R \rightarrow V} + \nu_D. \quad (32)$$

Apparently, the message mean is the same for all users as long as $\mu_{R \rightarrow V}$ and ν_D remain unchanged. We have proved that $\mu_{R \rightarrow V}$ remains unchanged with the proposed RCA and ν_D remains unchanged since we apply the same LDPC code for all users.

REFERENCES

- [1] C. Berrou and A. Glavieux, "Near optimum error correcting coding and decoding: turbo-codes," *IEEE Trans. Commun.*, vol. 44, no. 10, pp. 1261–1271, Oct. 1996.
- [2] T. J. Richardson, M. A. Shokrollahi, and R. L. Urbanke, "Design of capacity-approaching irregular low-density parity-check codes," *IEEE Trans. Inform. Theory*, vol. 47, no. 2, pp. 619–637, Feb. 2001.
- [3] E. Arıkan, "Channel Polarization: A Method for Constructing Capacity-Achieving Codes for Symmetric Binary-Input Memoryless Channels," *IEEE Trans. Inform. Theory*, vol. 55, no. 7, pp. 3051–3073, July 2009.
- [4] T. M. Cover and J. A. Thomas, *Elements of Information Theory*, 2nd ed. John Wiley & Sons, 2006.
- [5] T. Cover and C. Leung, "An achievable rate region for the multiple-access channel with feedback," *IEEE Trans. Inform. Theory*, vol. 27, no. 3, pp. 292–298, May 1981.
- [6] J. N. Laneman, D. N. C. Tse, and G. W. Wornell, "Cooperative diversity in wireless networks: Efficient protocols and outage behavior," *IEEE Trans. Inform. Theory*, vol. 50, no. 12, pp. 3062–3080, Dec. 2004.
- [7] Z. Ding, M. Peng, and H. V. Poor, "Cooperative Non-Orthogonal Multiple Access in 5G Systems," *IEEE Comm. Letters*, vol. 19, no. 8, pp. 1462–1465, Aug. 2015.
- [8] D. Tse and P. Viswanath, *Fundamentals of Wireless Communications*. Cambridge University Press, 2005.
- [9] G. Kramer, "Topics in multi-user information theory," *Foundations and Trends in Communications and Information Theory*, vol. 4, no. 4, pp. 265–444, 2008. [Online]. Available: <http://dx.doi.org/10.1561/01000000028>
- [10] J. Hou, J. E. Smee, H. D. Pfister, and S. Tomasin, "Implementing interference cancellation to increase the EV-DO Rev A reverse link capacity," *IEEE Comm. Mag.*, vol. 44, no. 2, pp. 58–64, Feb 2006.
- [11] Y. Hu and L. Ping, "Interleave-Division Multiple Access (IDMA)," in *Multiple Access Techniques for 5G Wireless Networks and Beyond*, M. Vaezi, Z. Ding, and H. V. Poor, Eds. Springer, 2019, ch. 13, pp. 417–449.
- [12] L. Dai, B. Wang, Y. Yuan, S. Han, C. I, and Z. Wang, "Non-orthogonal multiple access for 5G: solutions, challenges, opportunities, and future research trends," *IEEE Comm. Mag.*, vol. 53, no. 9, pp. 74–81, Sep. 2015.
- [13] Z. Ding, Y. Liu, J. Choi, Q. Sun, M. Elkashlan, C. I, and H. V. Poor, "Application of Non-Orthogonal Multiple Access in LTE and 5G Networks," *IEEE Comm. Mag.*, vol. 55, no. 2, pp. 185–191, Feb. 2017.
- [14] Y. Saito, Y. Kishiyama, A. Benjebbour, T. Nakamura, A. Li, and K. Higuchi, "Non-Orthogonal Multiple Access (NOMA) for Cellular Future Radio Access," in *2013 IEEE 77th Veh. Technol. Conf. (VTC Spring)*, June 2013, pp. 1–5.
- [15] Z. Ding, Z. Yang, P. Fan, and H. V. Poor, "On the Performance of Non-Orthogonal Multiple Access in 5G Systems with Randomly Deployed Users," *IEEE Sig. Process. Letters*, vol. 21, no. 12, pp. 1501–1505, Dec. 2014.

- [16] D. N. C. Tse and S. V. Hanly, "Multiaccess fading channels. i. polymatroid structure, optimal resource allocation and throughput capacities," *IEEE Trans. Inform. Theory*, vol. 44, no. 7, pp. 2796–2815, Nov. 1998.
- [17] L. Dai, B. Wang, Z. Ding, Z. Wang, S. Chen, and L. Hanzo, "A survey of non-orthogonal multiple access for 5g," *IEEE Commun. Surveys & Tutorials*, vol. 20, no. 3, pp. 2294–2323, thirdquarter 2018.
- [18] L. Ping, L. Liu, K. Y. Wu, and W. K. Leung, "Approaching the capacity of multiple access channels using interleaved low-rate codes," *IEEE Comm. Letters*, vol. 8, no. 1, pp. 4–6, Jan. 2004.
- [19] L. Ping, L. Liu, K. Wu, and W. K. Leung, "Interleave division multiple-access," *IEEE Trans. Wireless Commun.*, vol. 5, no. 4, pp. 938–947, April 2006.
- [20] P. A. Hoeher and H. Schoeneich, "Interleave-Division Multiple Access from a Multiuser Theory Point of View," in *4th Int. Symp. on Turbo Codes Related Topics; 6th Int. ITG-Conf. on Source and Channel Coding*, April 2006, pp. 1–5.
- [21] L. Liu, C. Yuen, Y. L. Guan, and Y. Li, "Capacity-achieving iterative LMMSE detection for MIMO-NOMA systems," in *2016 IEEE Int. Conf. on Commun. (ICC)*, May 2016, pp. 1–6.
- [22] L. Liu, Y. Chi, C. Yuen, Y. L. Guan, and Y. Li, "Capacity-achieving iterative LMMSE detection for MIMO-NOMA systems," *IEEE Trans. Signal Processing*, 2018.
- [23] Xiaodong Wang and H. V. Poor, "Iterative (turbo) soft interference cancellation and decoding for coded CDMA," *IEEE Trans. Commun.*, vol. 47, no. 7, pp. 1046–1061, July 1999.
- [24] S. ten Brink, G. Kramer, and A. Ashikhmin, "Design of low-density parity-check codes for modulation and detection," *IEEE Trans. Commun.*, vol. 52, no. 4, pp. 670–678, April 2004.
- [25] I. Andriyanova and J. P. Tillich, "Designing a Good Low-Rate Sparse-Graph Code," *IEEE Trans. Commun.*, vol. 60, no. 11, pp. 3181–3190, Nov. 2012.
- [26] J. Boutros and G. Caire, "Iterative multiuser joint decoding: unified framework and asymptotic analysis," *IEEE Trans. Inform. Theory*, vol. 48, no. 7, pp. 1772–1793, July 2002.
- [27] G. Caire, R. R. Muller, and T. Tanaka, "Iterative multiuser joint decoding: optimal power allocation and low-complexity implementation," *IEEE Trans. Inform. Theory*, vol. 50, no. 9, pp. 1950–1973, Sep. 2004.
- [28] K. Li and X. Wang, "EXIT chart analysis of turbo multiuser detection," *IEEE Trans. Wireless Commun.*, vol. 4, no. 1, pp. 300–311, Jan. 2005.
- [29] K. Li, X. Wang, and L. Ping, "Analysis and Optimization of Interleave-Division Multiple-Access Communication Systems," *IEEE Trans. Wireless Commun.*, vol. 6, no. 5, pp. 1973–1983, May 2007.
- [30] L. Liu, J. Tong, and L. Ping, "Analysis and optimization of CDMA systems with chip-level interleavers," *IEEE J. Sel. Areas Commun.*, vol. 24, no. 1, pp. 141–150, Jan. 2006.
- [31] S. ten Brink, "Convergence behavior of iteratively decoded parallel concatenated codes," *IEEE Trans. Commun.*, vol. 49, no. 10, pp. 1727–1737, Oct. 2001.
- [32] R. Zhang and L. Hanzo, "EXIT Chart Based Joint Code-Rate and Spreading-Factor Optimisation of Single-Carrier Interleave Division Multiple Access," in *2007 IEEE Wireless Commun. and Networking Conf.*, March 2007, pp. 735–739.
- [33] R. Zhang, L. Xu, S. Chen, and L. Hanzo, "EXIT-Chart-Aided Hybrid Multiuser Detector for Multicarrier Interleave-Division Multiple Access," *IEEE Trans. Veh. Technol.*, vol. 59, no. 3, pp. 1563–1567, March 2010.
- [34] A. Balatsoukas-Stimming and A. P. Liavas, "Design of LDPC Codes for the Unequal Power Two-User Gaussian Multiple Access Channel," *IEEE Wireless Comm. Letters*, vol. 7, no. 5, pp. 868–871, Oct. 2018.
- [35] J. Du, L. Zhou, L. Yang, S. Peng, and J. Yuan, "A New LDPC Coded Scheme for Two-User Gaussian Multiple Access Channels," *IEEE Comm. Letters*, vol. 22, no. 1, pp. 21–24, Jan. 2018.
- [36] S. Sharifi, A. K. Tanc, and T. M. Duman, "LDPC Code Design for the Two-User Gaussian Multiple Access Channel," *IEEE Trans. Wireless Commun.*, vol. 15, no. 4, pp. 2833–2844, April 2016.
- [37] Y. Zhang, K. Peng, and J. Song, "Enhanced IDMA with Rate-Compatible Raptor-Like Quasi-Cyclic LDPC Code for 5G," in *2017 IEEE Globecom Workshops (GC Wkshps)*, Dec. 2017, pp. 1–6.
- [38] Y. Zhang, K. Peng, X. Wang, and J. Song, "Performance Analysis and Code Optimization of IDMA With 5G New Radio LDPC Code," *IEEE Comm. Letters*, vol. 22, no. 8, pp. 1552–1555, Aug. 2018.
- [39] L. Schmalen and S. ten Brink, "Combining Spatially Coupled LDPC Codes with Modulation and Detection," in *SCC 2013; 9th Int. ITG Conf. on Syst., Commun. and Coding*, Jan. 2013, pp. 1–6.
- [40] S. Cammerer, L. Schmalen, V. Aref, and S. ten Brink, "Wave-like decoding of tail-biting spatially coupled LDPC codes through iterative demapping," in *2016 9th Int. Symp. on Turbo Codes and Iterative Inform. Process. (ISTC)*, Sept. 2016, pp. 121–125.
- [41] G. Song and J. Cheng, "Distance enumerator analysis for interleave-division multi-user codes," *IEEE Trans. Inform. Theory*, vol. 62, no. 7, pp. 4039–4053, July 2016.
- [42] —, "Low-complexity coding scheme to approach multiple-access channel capacity," in *2015 IEEE Int. Symp. on Inform. Theory (ISIT)*, June 2015, pp. 2106–2110.
- [43] Y. Hu, C. Liang, J. Hu, and L. Ping, "Low-cost implementation techniques for interleave division multiple access," *IEEE Comm. Letters*, pp. 1026–1029, June 2018.
- [44] Y. Hu, C. Liang, L. Liu, C. Yan, Y. Yuan, and L. Ping, "Interleave-division multiple access in high rate applications," *IEEE Comm. Letters*, Oct. 2018.
- [45] D. Guo, S. Shamai, and S. Verdú, "Mutual information and minimum mean-square error in Gaussian channels," *IEEE Trans. Inform. Theory*, vol. 51, no. 4, pp. 1261–1282, April 2005.
- [46] K. Kusume, G. Bauch, and W. Utschick, "IDMA vs. CDMA: Analysis and Comparison of Two Multiple Access Schemes," *IEEE Trans. Wireless Commun.*, vol. 11, no. 1, pp. 78–87, Jan. 2012.
- [47] S. Cammerer, X. Wang, Y. Ma, and S. ten Brink, "Spatially coupled LDPC codes and the multiple access channel," in *2019 53rd Annual Conference on Information Sciences and Systems (CISS)*, March 2019, pp. 1–6.
- [48] F. Brännstrom, L. K. Rasmussen, and A. J. Grant, "Convergence Analysis and Optimal Scheduling for Multiple Concatenated Codes," *IEEE Trans. Inform. Theory*, vol. 51, no. 9, pp. 3354–3364, Sept. 2005.
- [49] Sae-Young Chung, T. J. Richardson, and R. L. Urbanke, "Analysis of sum-product decoding of low-density parity-check codes using a Gaussian approximation," *IEEE Trans. Inform. Theory*, vol. 47, no. 2, pp. 657–670, Feb 2001.
- [50] X.-Y. Hu, E. Eleftheriou, and D. M. Arnold, "Regular and Irregular Progressive Edge-Growth Tanner Graphs," *IEEE Trans. Inform. Theory*, vol. 51, no. 1, pp. 386–398, Jan. 2005.
- [51] G. Liva, S. Song, L. Lan, Y. Zhang, S. Lin, and W. E. Ryan, "Design of LDPC Codes: A Survey and New Results," *J. Commun. Software Syst.*, vol. 2, no. 3, p. 191, Sep. 2006.
- [52] X. Wang. (2018) IDMA LDPC Parity Check Matrices. [Online]. Available: https://github.com/xjewang/IDMA_LDPC_codes